AIChE

SMB Chromatography Design Using Profile Advancement Factors, Miniplant Data, and Rate-Based Process Simulation

Shawn D. Feist
Engineering and Process Sciences Laboratory, The Dow Chemical Company, Midland, MI 48667

Yogesh Hasabnis
Engineering and Process Sciences Laboratory, Dow Chemical International Pvt. Ltd., Pune, India

Bruce W. Pynnonen
Dow Water and Process Solutions, Larkin Laboratory, The Dow Chemical Company, Midland, MI 48674

Timothy C. Frank
Engineering and Process Sciences Laboratory, The Dow Chemical Company, Midland, MI 48667

DOI 10.1002/aic.11938
Published online August 13, 2009 in Wiley InterScience (www.interscience.wiley.com).

This article describes a systematic miniplant-based approach to rapid development of simulated moving bed (SMB) chromatography applications. The methodology involves analysis of single-column pulse tests to screen adsorbents and operating conditions and to determine initial values of profile advancement factors used to specify flow rates for an initial SMB miniplant experiment. A lumped-parameter linear driving force rate-based model is developed by fitting process data from a single miniplant run. The data are fit in a two-step procedure involving initial determination of effective adsorption isotherm constants as best-fit parameters with subsequent adjustment of calculated mass transfer coefficients to refine the data fit. The resulting simulation is used to guide further miniplant work and minimize experimental effort. The methodology is illustrated with miniplant data for a binary protein separation showing excellent agreement between model results and process data generated over a wide range of operating conditions. © 2009 American Institute of Chemical Engineers *AIChE J,* 55: 2848–2860, 2009

Keywords: simulated moving bed, chromatography, process simulation, process development, process design, separation, purification

Introduction

Miniplants have long been utilized in the design of separation processes for chemical manufacturing.[1] The miniplant is a scaled-down version of the equipment envisioned for the commercial scale. It is sized for reasonably small feed volumes and to allow convenient modification for rapid evaluation of potential improvements, yet the scale should be sufficiently large to allow reliable scale-up. Ideally, this approach to specifying a commercial design should be combined with computer simulation to correlate performance data in terms of fundamental relationships between process variables. The resulting model can then be used to guide further experimentation and ultimately to develop a mathematical framework

Correspondence concerning this article should be addressed to T. C. Frank at tcfrank@dow.com.

for design calculations.[2] This combined approach is routinely employed when specifying operating conditions and equipment dimensions for commercial processes involving distillation[3–5] and liquid–liquid extraction.[5–7]

In the present work, we show how the miniplant concept in combination with process simulation can provide an efficient methodology for developing simulated moving bed (SMB) chromatography applications and for demonstrating a functioning design at the miniplant scale. In our work, we have found that computer simulations generally are not sufficiently accurate to eliminate miniplant experimentation altogether, although they are very valuable for identifying trends and thus for reducing the number of miniplant experiments. Once satisfactory performance has been demonstrated in the miniplant and favorable process economics have been established, the focus can turn to scaling up the design to achieve the same performance at the commercial scale. Methods for scale-up of fixed-bed adsorption and chromatography equipment are described elsewhere.[8–12]

The advantages of a simulated moving bed (SMB) process scheme compared to standard or batch elution chromatography include the ability to minimize dilution of products and maximize the productivity of the separation media while achieving high purity and recovery of the desired product or products.[8,13–15] The basic SMB process was patented in 1961 by Broughton and Gerhold at UOP.[13] It was first commercialized for purification of *p*-xylene[16] and has since been developed in a variety of forms for other applications. One of the best known involves separation of fructose and glucose to produce enriched high-fructose corn syrup.[17] The use of ion-exchange media for this separation was first described by Lefevre[18] at Dow in 1962, and SMB technology was later employed to improve process productivity. More recently, a great deal of attention has been given to separation of specialty chemicals including therapeutic proteins and other biomolecules[19–21] and chiral compounds.[22–25] To facilitate evaluation of additional applications where SMB chromatography may provide a cost effective option and thus take full advantage of its potential, new methods are needed that allow rapid assessment of process feasibility and rapid specification of reliable designs where appropriate, and this is the focus of our work.

A method involving analysis of single-column pulse tests to determine approximate operating conditions for a new SMB chromatography application was first published by deRosset et al. in 1976.[26] A number of authors have since proposed methods for optimizing SMB performance.[22–25,27–30] In our process design work, we have introduced the use of profile advancement factors obtained from pulse tests and emphasized generation of key miniplant data to quickly develop an accurate simulation. To illustrate the methodology, we chose the protein separation studied by Houwing et al.[20] as a model system. This system, which is not of commercial interest, involves separation of aqueous bovine serum albumin (BSA) from equine heart myoglobin (EHM).

Key process concepts

A typical SMB process employs multiple fixed-bed columns (or sections of columns) and four zones to separate feed solutes into two fractions: a slow-eluting fraction in the extract and a fast-eluting fraction in the raffinate.[8,9,15] In the model system we chose to study, BSA is the fast eluter (66 kDa molecular size) and EHM is the slow eluter (17 kDa). The SMB process is operated by switching the flow of liquids from one column to another (or between column sections) to approach the theoretical performance of true countercurrent solid–liquid flow. Compared to true countercurrent operation, the somewhat-less efficient SMB fixed-bed mode of operation avoids problems associated with engineering the movement of solids. In this section, we review key definitions of SMB process productivity and describe strategies for increasing productivity.

Process Productivity. The productivity of an SMB process often is expressed in terms of the production rate per total packed-bed volume (P_{media}, a measure of media utilization efficiency) or in terms of the mass of product produced per volume of feed plus elution solvent (P_{solvent}, a measure of solvent usage efficiency):

$$P_{\text{media}} = \frac{C_{\text{A,raff}} Q_{\text{raff}} + C_{\text{B,extract}} Q_{\text{extract}}}{V_{\text{media}}} \tag{1}$$

$$P_{\text{solvent}} = \frac{C_{\text{A,raff}} Q_{\text{raff}} + C_{\text{B,extract}} Q_{\text{extract}}}{Q_{\text{feed}} + Q_{\text{eluent}}} \tag{2}$$

In these equations, solute A is a relatively fast eluting product isolated in the raffinate, and solute B is a slower eluting product isolated in the extract. Productivity also may be defined for a single product solute A or B, in which case only the term corresponding to the solute of interest appears in the numerators of Eqs. 1 and 2. Additionally, a product dilution factor may be defined for each key product solute:

$$F_{\text{dilution.A}} = \frac{C_{\text{A,feed}}}{C_{\text{A,raff}}} \tag{3}$$

$$F_{\text{dilution.B}} = \frac{C_{\text{B,feed}}}{C_{\text{B,extract}}} \tag{4}$$

Process Zones. A four-zone SMB process scheme is illustrated in Figure 1. The four zones form an internal loop. Liquid flow rates and step time are adjusted so that key slow and fast eluting solutes move in opposite directions relative to the movement or switching of inlet and outlet ports through the loop's sequence. Zone I is located from the eluent inlet to the extract outlet; Zone II is between the extract outlet and the feed inlet; Zone III is between the feed inlet and raffinate outlet; and Zone IV is between the raffinate outlet and the eluent inlet. Within the SMB loop, Zones II and III serve to allow the key fast and slow components to move farther apart, while Zones I and IV serve to prevent the slow component from falling too far back and the fast component from moving too far forward, respectively. For this study, the 12 SMB columns were allocated in a 2-5-4-1 zone configuration as follows: 2 columns in Zone I; 5 columns in Zone II; 4 columns in Zones III; and 1 column in Zone IV. Because the bulk of the separation in an SMB process occurs in Zones II and III, more of the columns were allocated to these zones.

Flow Rate Requirements. For high productivity operation, liquid flow rates must be carefully adjusted to improve the separation while minimizing solvent consumption. As an extreme example, if the flow rates in all of the zones were

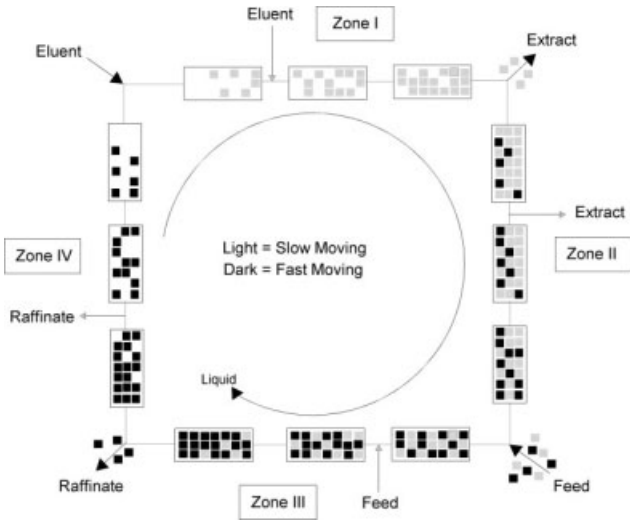

Figure 1. Four-zone SMB operation.

the same, the key fast eluter would continue to move net "forward" (clockwise in Figure 1), while the key slow eluter would continue to move net "backward" (counterclockwise in Figure 1). Eventually, the fast eluter would lap the slow eluter such that the two components become mixed together at a lower concentration than present in the feed stream. In general, flow rates must be adjusted to prevent the components from lapping each other and to generate an internal profile in which essentially all of the fast eluter exits in the raffinate and all of the slow eluter exits in the extract.

In Zone II, the ideal flow rate is such that the fast eluter barely moves forward (clockwise into Zone III). Consequently, the flow rate in Zone II is not fast enough to allow the majority of the slow eluter to move forward. In Zone III, the liquid flow rate is chosen so that the slow eluter barely moves backward (counterclockwise) and thus the fast eluter will continue to move forward. The liquid flow rate in Zone III will always be greater than the flow rate in Zone II because the flow rate in Zone III is equal to the sum of the flow rates of Zone II and the entering feed.

Much has been published on identifying proper flow rates for Zones II and III; this is the main focus of the triangle theory of SMB operation.[31] However, flow rates for Zones IV and I also are critical to achieving economically viable, highly productive operation. In these two SMB zones, the lowest and highest flow rates are used, respectively. In Zone IV, where the key fast eluter is prevented from lapping the key slower eluter, the flow rate should be adjusted so that even the fast eluter is forced in the backward direction and the flow rate is just slow enough to prevent the fast eluter from moving from Zone IV into Zone I. The flow rate in Zone IV should be no slower than necessary because this yields a more economical operation as more solvent will be recycled into Zone I and less fresh solvent will be required. In Zone I, where the key slow eluter is prevented from falling behind, the flow rate should be adjusted so that it is just fast enough to force the slow eluter to move forward; that is, to prevent it from falling backward from Zone I into Zone IV. Specifying a flow rate in Zone IV that is too slow or a flow rate in Zone I that is too fast requires extra elution solvent and reduces the efficiency of the SMB process.

Experimental and Simulation Details

Materials

Proteins were obtained from Sigma Aldrich: bovine serum albumin (BSA), 66 kDa, pH ~7, $\geq$ 98% purity (catalog no. A7906); and equine heart myoglobin (EHM), 17 kDa, $\geq$ 90% purity (catalog no. M1882). Deionized water (containing 0.15 M NaCl and 10 mM phosphate buffer) was used for feed and elution solvent. The chromatography media were Perloza® MT 100 Medium macroporous spherical cellulose beads manufactured by Iontosorb (www.iontosorb.cz, Czech Republic). Bead diameters were 100–250 μm, with a volume median diameter of 175 μm. A previous study[32] reported very high particle porosity, $\varepsilon_p = 0.919$. The manufacturer has reported fractions of total pore volume accessible by bovine serum albumin and by myoglobin equal to 0.70 and 0.83, respectively.

Apparatus

The SMB miniplant was a Knauer GmbH model CSEP® C912 apparatus controlled using ValveChrom® software. The miniplant contained 12 stainless steel columns, each 36 inches (0.91 m) long with a 0.43 inch (1.09 cm) inner diameter. The inner diameter was sufficiently large to avoid significant wall effects. Column ends were fitted with 0.5-inch OptiFlow® end-fittings and distributor from Grace Davison, and an 80-μm screen. Each column was packed using media slurried in eluent containing 10 mM phosphate buffer with a higher NaCl concentration than that used later during operation (0.2 M NaCl vs. 0.15 M NaCl). Using a somewhat more concentrated salt solution caused the media to shrink slightly; packing each column this way allowed the media to expand slightly once the columns were put into operation, thus minimizing formation of excess void spaces. The 12 columns were mounted on the Knauer system's rotating carousel housed in a 25°C air-heated oven. The total volume of the 12 columns (or total media volume) was 1028 mL. Total system volume including dead volume between columns was estimated to be about 1040 mL. Feed and elution-solvent supply tanks, and extract and raffinate receivers, were placed on electronic balances so the inlet and outlet mass flow rates and overall material balance could be monitored.

Operating and sampling procedures

The miniplant was operated at constant flow rates for feed and elution solvent and for removal of raffinate and extract from the SMB loop. Flow rates were calibrated using elution solvent and then monitored during miniplant operation by measuring weight changes for feed, elution solvent, raffinate, and extract. Flow rates typically varied within $\pm$5% for the feed flow rate and within $\pm$2% for all other flows. For plotting internal process concentration profiles, 1 mL samples of liquid exiting a single column were taken at the start of each step in a 12-step cycle using an 8-port sampling valve from Valco Instruments (model 8UW). Achieving steady cyclical operation generally required 12 complete cycles or about 1.2 days of run time. After steady operation had been achieved, composite samples of raffinate and of extract were collected through an entire 12-step cycle.

Analytical

Samples were analyzed using an Agilent 1100 Series HPLC equipped with an autosampler, a UV detector (220 nm), and a Zorbax® 3000SB-C3 column (4.6 × 150 mm^2, 5-μm particle diameter) at 25°C. A gradient analytical method was controlled using ChemStation® software. Mobile phase A was HPLC grade water with 0.1 vol % trifluoroacetic acid. Mobile phase B was HPLC grade acetonitrile with 0.085 vol % trifluoroacetic acid. The flow rate was 1.0 mL/min. Over a 10-min period, the mobile phase composition was changed linearly from 65% A/35% B to 25% A/75% B, after which the composition was changed back to the starting composition and the column re-equilibrated for 8 min prior to the next injection. The sample injection volume was 10 μL. Reported concentrations are the average values of two analyses.

Process simulation

Lumped-Parameter Model. A number of approaches have been taken to analyze or simulate SMB process schemes including the use of true moving bed approximations[14,33] and standing-wave models.[29,33] In our work, we utilized a standard lumped-parameter linear driving force rate-based model.[14,20,21,34,35] With this approach, the material balance for component i in column j, in terms of mass per unit volume, is given by

$$\varepsilon_b \frac{\partial C_{ij}}{\partial t} = \varepsilon_b E_j \frac{\partial^2 C_{ij}}{\partial x^2} - u_j \frac{\partial C_{ij}}{\partial x} - (1-\varepsilon_b) k_{m,i} a_p \left(q_{ij}^{eq} - q_{ij}\right) \tag{5}$$

The material balance within a solid particle is

$$\frac{\partial q_{ij}}{\partial t} = k_{m,i} a_p \left(q_{ij}^{eq} - q_{ij}\right) \tag{6}$$

The lumped-parameter or overall mass transfer coefficient ($k_{m,i}$) is related to individual mass transfer coefficients through the reciprocal addition rule:

$$\frac{1}{k_{m,i}} = \frac{K_i}{k_{ext,i}} + \frac{K_i}{k_{int,i}} \approx \frac{K_i}{k_{int,i}} \tag{7}$$

where $k_{ext,i}$ accounts for mass transfer at the external surface of a particle and $k_{int,i}$ accounts for mass transfer within the pores. Values for $k_{ext,i}$ may be obtained from various correlation equations[36–38]; however, for most liquid chromatography applications the overall rate of mass transfer is controlled by resistance within the pores, so the $k_{ext,i}$ term can be neglected. Values for $k_{int,i}$ may be estimated from well-known expressions for intraparticle mass transfer,[21,36–38] yielding the following approximate equation:

$$k_{m,i} \approx \frac{k_{int,i}}{K_i} \approx \frac{10 D_{eff,i}}{K_i d_p} \approx \frac{10}{K_i d_p} \frac{(F_{se,i}\varepsilon_p)^2 D_{m,i}}{(2 - F_{se,i}\varepsilon_p)^2} \tag{8}$$

In utilizing Eqs. 7 and 8, it is assumed that the system exhibits near-linear isotherm behavior and that diffusion within macropores provides the dominant resistance to mass transfer.[21,35,38] We have included a size exclusion factor ($F_{se,i}$) to represent the fraction of internal porosity that can be accessed by a given solute. Specifying linear isotherms

$$q_{ij}^{eq} = K_i C_{ij} \tag{9}$$

and substituting $a_p = 6/d_p$ for uniform spherical particles, Eqs. 5 and 6 may then be expressed as follows:

$$\frac{\partial C_{ij}}{\partial t} = E_j \frac{\partial^2 C_{ij}}{\partial x^2} - \frac{u_j}{\varepsilon_b}\frac{\partial C_{ij}}{\partial x} - \psi_i \left(\frac{1-\varepsilon_b}{\varepsilon_b}\right) C_{ij} + \frac{\psi_i}{K_i}\left(\frac{1-\varepsilon_b}{\varepsilon_b}\right) q_{ij} \tag{10}$$

$$\frac{\partial q_{ij}}{\partial t} = \psi_i C_{ij} - \frac{\psi_i}{K_i} q_{ij} \tag{11}$$

where the symbol ψ_i denotes constants for each solute given by

$$\psi_i = k_{m,i} a_p K_i \approx k_{int,i} a_p \approx \frac{(F_{se,i}\varepsilon_p)^2}{(2 - F_{se,i}\varepsilon_p)^2} \frac{60 D_{m,i}}{d_p^2} \tag{12}$$

Equation 12 allows estimation of mass transfer resistance independent of K_i and without detailed characterization of the media's internal pore structure.

The approximations inherent in Eqs. 10–12, in addition to those described earlier, include the following: (1) particle size distribution is nearly uniform or can be represented by a single effective diameter; (2) mass transfer coefficients are independent of solute concentration and liquid velocity; (3) equilibrium adsorption capacity remains a linear function of solute concentration and does not approach saturation at high solute concentrations; (4) adsorption and mass transfer effects for any one component in a multicomponent system are independent of other components; and (5) the operation is isothermal with negligible thermal effects due to adsorption. In addition, the use of F_{se} to account for any size exclusion effects provides only a rough approximation. A term accounting for the spreading of concentration profiles due to dead volume between columns, as described by Migliorini et al.,[39] was not included because the amount of dead volume within our miniplant system was negligible (<1.2%).

Boundary Conditions. The SMB boundary conditions are given by

$$C_{ij} - \frac{E_j}{v_j}\frac{\partial C_{ij}}{\partial x} = C_{i,0} \text{ at } x = 0 \tag{13}$$

$$\text{Extract node, } C_{ij} = C_{ij+1,0} \text{ at } x = L \tag{14}$$

$$\text{Raffinate node, } C_{ij} = C_{ij+1,0} \text{ at } x = L \tag{15}$$

$$\text{Eluent node, } C_{ij} = \frac{Q_I}{Q_{IV}} C_{ij+1,0} \text{ at } x = L \tag{16}$$

$$\text{Feed node, } C_{ij} = \frac{Q_{III}}{Q_{II}} C_{ij+1.0} - \frac{Q_{feed}}{Q_{II}} C_{i,feed} \text{ at } x = L \tag{17}$$

The overall flow balances are

$$\text{Extract node, } Q_{\text{II}} = Q_{\text{I}} - Q_{\text{extract}} \quad (18)$$

$$\text{Raffinate node, } Q_{\text{IV}} = Q_{\text{III}} - Q_{\text{raff}} \quad (19)$$

$$\text{Eluent node, } Q_{\text{I}} = Q_{\text{IV}} + Q_{\text{eluent}} \quad (20)$$

$$\text{Feed node, } Q_{\text{III}} = Q_{\text{II}} + Q_{\text{feed}} \quad (21)$$

For our work, solute concentrations were set to zero everywhere at time zero.

Determining Suitable Parameter Values. Axial dispersion coefficients E_j may be calculated by using the data correlation of Chung and Wen[40]:

$$Pe = \frac{d_{\text{p}} u_j}{E_j} = 0.2 + 0.011 Re^{0.48} \quad (22)$$

An average particle diameter (for which $a_{\text{p}} \approx 6/d_{\text{p}}$) must be estimated from knowledge of the media. We chose to represent the Perloza® MT 100 particle size distribution (100–250 μm) by using the volume mean diameter of 175 μm. For ε_{b}, a value of 0.35 is recommended for spherical media of near uniform size distribution. Somewhat smaller values may result for well-packed spherical media with a significant fraction of relatively small particles. Irregularly shaped particles often exhibit values of $\varepsilon_{\text{b}} = 0.4$–0.5. The actual value will also depend on the procedures used to pack a given column.[37] Molecular diffusivities may be estimated from the Siddiqi and Lucas correlations[41]:

$$D_{\text{m},i} = 2.98 \times 10^{-7} \frac{T}{\mu^{1.026} V_{\text{m},i}^{0.5473}}, \text{ for aqueous solutions} \quad (23)$$

$$D_{\text{m},i} = 9.89 \times 10^{-8} \frac{V_{\text{m.liquid}}^{0.265} T}{\mu^{0.907} V_{\text{m},i}^{0.45}}, \text{ for organic solutions} \quad (24)$$

using the following units: $D_{\text{m},i}$ in cm^2/s, T in K, $V_{\text{m,liquid}}$ and $V_{\text{m},i}$ in mL/g mol, and μ in cP. Values for ε_{p} and $F_{\text{se},i}$ must be determined from measurements or estimated by comparison with similar materials.

To obtain effective values for mass transfer coefficients and isotherm constants, we propose the following two-step procedure: (1) calculate initial values for $\psi_i = k_{\text{int},i}\, a_{\text{p}}$ from Eq. 12 and determine effective values for K_i by fitting available SMB process data, treating the K_i values as adjustable parameters; and (2) refine the values for the mass transfer coefficients by refitting the data, now treating the ψ_i values as adjustable parameters while maintaining the K_i values as constants. Note that in using this approach, only approximate values of ε_{b}, ε_{p}, $F_{\text{se},i}$, $D_{\text{m},i}$, and d_{p} are needed because by adjusting K_i and ψ_i to match process data the methodology compensates for uncertainties in these system properties. The resulting best-fit values also represent overall values that compensate to some extent for approximations inherent in the model's derivation. Alternatively, isotherm constants and mass transfer coefficients could be determined by careful measurement of liquid–solid equilibrium and solute diffusivities, or one might extract these parameter values from analysis of chromatograms or pulse tests.[36,42,43] We prefer to determine effective values by fitting actual SMB process data, because this insures a process simulation that is sufficiently accurate for process design purposes.

Computer Methods. Athena Visual Studio® software[44,45] was used to solve the model's system of partial differential equations, employing the upwind second order WENO method[46] and PDAPLUS Solver. The calculations were carried out for 12 cycles of SMB operation to insure a good representation of steady cyclical operation (where a single cycle refers to 12 step changes) using 600 discrete position calculation points (50 increments for each column in the column concentration profile) and 100,000 total discretization points with respect to time (giving a time increment of $\sim$1 s). This was necessary to insure that the material balances for each solute in the raffinate and extract closed reasonably well (generally within 100 $\pm$ 2%). The material balance was determined by comparing $C_{\text{A,feed}} Q_{\text{feed}}$ with $C_{\text{A,raff}} Q_{\text{raff}} + C_{\text{A,extract}} Q_{\text{extract}}$ for solute A (and the corresponding comparison for solute B). Additional numerical accuracy was possible, but this required using a larger number of calculation points which added considerably to the required computation time. Using a PC with 2.6 GHz processor and 2.0 GB RAM, the typical computation time for a single computer run was on the order of 10 h. Additional discussion of material balance errors and computation time for rate-based SMB simulation is given elsewhere.[47]

Because of long computation times, we did not attempt to precisely quantify the effects that uncertainties in the various input values had on calculated outputs. One possible approach for future study is given by Xin and Whiting.[48] These authors have proposed a general Monte Carlo methodology that requires evaluation of 100+ simulations to determine the range of uncertainties in simulation results for known (or estimated) uncertainties in input values.

Results and Discussion

Determining SMB start-up conditions from pulse tests

Pulse test data were generated using a single miniplant-size column packed with Perloza® MT 100 Medium media (Figure 2). The data are expressed in terms of solute concentration in the effluent relative to that in the feed ($C_{i,\text{effluent}}/C_{i,\text{feed}}$) versus the number of empty bed volumes (BV) of feed liquid that have passed through the column. These are convenient treatments to normalize the data with respect to feed concentration and column size. The data in Figure 2 were used to select values of profile advancement factors given by

$$f_{\text{k}} = \frac{Q_{\text{k}} t_{\text{step}}}{V_{\text{column}}} \quad (25)$$

using the logic outlined in Table 1. The resulting f_{k} values were used to set target flow rates for the first SMB miniplant run. The analysis of Figure 2 is summarized in Tables 2 and 3. This approach to determining SMB starting conditions was developed at Dow by Pynnonen.[49] It is an extension of the pulse test methodology introduced by DeRosset et al.[26] and utilizes concepts similar to triangle theory.[31]

The logic of Table 1 and Eq. 25 can be stated as follows: By requiring that $f_{\text{k}} = \text{BV}_{\text{j}} = Q_{\text{k}} \times t_{\text{step}}/V_{\text{column}}$, one is setting the advancement of solutes within a column to be equal

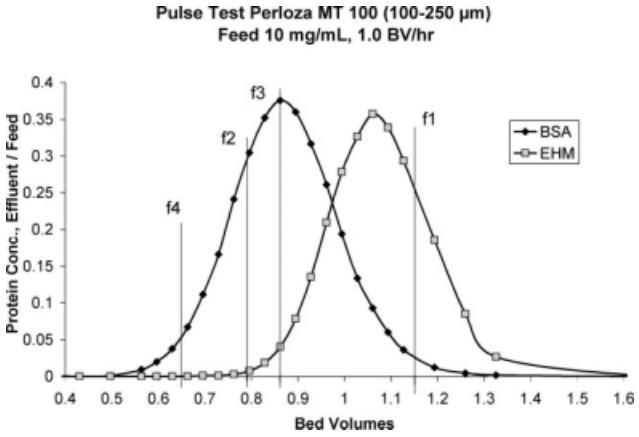

Figure 2. Pulse test results used to generate initial SMB run parameters.

Conditions: Temp. = 22°C; protein concentration in the feed pulse = 10 g/L protein (50% BSL, 50% EHM); media = Perloza MT 100 Medium beads; inlet flow rate = 1.0 bed volume per hour; face velocity = 1.5 cm/min.

to (or nearly equal to) that measured in the pulse test, at the point where the desired effect is achieved (as described in Table 1), because the test is carried out using a single column of the same size packed with the same media. The use of multiple columns within a zone improves the separation by allowing components to move farther apart. Once initial values for f_3, f_4, and f_1 are chosen by interpretation of the pulse test data and the maximum face velocity was specified, then all the flow rates plus values for f_2 and t_{step} can be determined from the material balance for the process (Eqs. 18–21) and Eq. 25.

In our example, the pulse test was conducted at a face velocity of 1.5 cm/min. Face velocities will not be the same in the SMB run, and indeed will be different in each zone, but they do not need to be exactly the same because the pulse test data are normalized. Concentration profiles likely will change somewhat over a range of flow rates due to mass-transfer resistance effects, but the pulse test analysis provides a good initial measure of what can be expected. Also note that the pulse test data in Figure 2 do not show baseline resolution between the component peaks nor is this desirable. Instead, the goal is to separate the leading edge of one peak (the fast eluter) from the trailing edge of the other peak (the slow eluter). The peaks should overlap significantly while maintaining good purities within the leading edge and trailing edge regions; that is, without significant peak spreading. This facilitates a good binary separation at the maximum productivity potential. If the overlap is small, the concentration of solute in the feed pulse should be increased and the test repeated.

Miniplant results

A total of seven sequential runs were made using the SMB miniplant. Decisions to adjust each run were made by evaluating the internal component profiles and adjusting the four profile advancement factors using the logic outlined in Table 1 and described in Process Concepts. The miniplant data were later used to evaluate our approach to process modeling. Liquid face velocities (the superficial liquid velocities at the entrance to each column) for all Runs, and the corresponding profile advancement factors, are listed in Table 2. The miniplant operating conditions are summarized in Table 3. The process concentration profiles obtained for each run are shown in Figures 3–6. These are standard plots showing solute concentrations sampled at the beginning of each step as a function of column sequence number (the position relative to the beginning of Zone I). Brackets with labels are included to indicate where feed and elution solvent were added to the process and where raffinate and extract were removed from the process. Careful accounting for concentrations over the ranges where extract and raffinate exit the SMB loop is particularly important, because the concentrations of solute in these streams change greatly over the course of a step and because the integrated concentrations give the process product compositions which are used to calculate system performance.

Product concentrations, purities, and recoveries are listed in Table 4 for each run. The concentrations are the composite values for an entire cycle (12 steps). Recoveries were

Table 1. Selection of Initial Profile Advancement Factors by Analysis of Pulse Test Data*

1	Start by specifying f_3 for Zone III. From the chromatogram, choose a BV value that includes a large fraction of fast eluter, but only a small fraction of slow eluter (at the leading edge of the second peak). The goal is to choose a value that achieves high recovery of fast eluter in the raffinate while minimizing the amount of slow eluter that contaminates the raffinate. Set f_3 equal to this value.
2	Specify f_4 for Zone IV. Choose a BV value that includes some of the fast eluter but only a small fraction of this component (at the leading edge of the first peak). The goal is to choose a value that prevents fast eluter from moving forward into Zone I, but is as large as possible to minimize the required amount of fresh elution solvent that needs to be added to Zone I. Set f_4 equal to this value.
3	Specify f_1 for Zone I. Choose a BV value that includes a majority of the slow eluter and almost all of the fast eluter (at the trailing edge of the first peak). The goal is to choose a value that prevents slow eluter from falling back into Zone IV, but is as small as possible to minimize the required amount of elution solvent. Set f_1 equal to this value. Note: This procedure can be visualized as the mirror image of the procedure used to select f_3, by interpreting the chromatogram from right to left instead of left to right.
4	Choose a maximum face velocity. Specify a value no greater than about 10 cm/min (about 3 gallons per minute per ft^2 of cross-sectional area) for any one of the columns, unless data are available for similar systems suggesting larger values are likely to be appropriate. Alternatively, a study of face velocity effects may be conducted in the course of running pulse tests.
5	Calculate flow rates for all the process streams and zones by material balance using Eqs. 18–21 and 25. This also sets the values of f_2 and t_{step}. Note that $f_4 < f_2 < f_3 < f_1$, consistent with triangle theory.[31]

*Refer to Figures 1 and 2 and to Key Process Concepts for discussion of each zone and its function.

Table 2. Face Velocities and Profile Advancement Factors

Run	Zone I Liquid Face Velocity (cm/min)	Zone II Liquid Face Velocity (cm/min)	Zone III Liquid Face Velocity (cm/min)	Zone IV Liquid Face Velocity (cm/min)	Profile Advancement Factors			
					f_1	f_2	f_3	f_4
Run 1 target*	8.1	5.5	6.1	4.5	1.15	0.78	0.86	0.64
Run 1 actual†	8.0	5.6	6.1	4.6	1.135	0.795	0.870	0.653
Run 2	8.0	5.6	6.1	4.6	1.222	0.856	0.932	0.703
Run 3	8.0	5.6	6.1	4.6	1.310	0.916	1.003	0.753
Run 4	7.7	5.6	6.1	4.3	1.257	0.917	1.003	0.700
Run 5	7.9	5.8	6.3	4.1	1.237	0.913	0.995	0.639
Run 6	7.9	5.8	6.4	4.1	1.244	0.915	0.997	0.639
Run 7	15.8	11.7	12.7	8.1	1.237	0.916	0.997	0.639

*Target conditions estimated from pulse test data (Figure 2).
†Conditions obtained after minor adjustments made during the run.

calculated two ways: (1) as calculated directly from the analytical results, and (2) as adjusted to force 100% accountability for each protein. The experimental accountability for each solute typically was within 100 ± 5%. In those cases where experimental accountability was greater than 100%, forcing closure of the material balance resulted in a smaller reported recovery value. Most likely, these differences are due to small errors in flow rate measurements; however, they may also be due to small errors in measuring protein concentrations.

After the initial shakedown run, each subsequent run involved an adjustment in operating conditions to move toward improved performance. In Runs 2–5, the profile advancement factors were adjusted slightly in each run by changing flow rates and/or steptimes to move the operation toward achieving higher purities and recoveries, keeping in mind the flow rate requirements outlined earlier in Key Process Concepts. In Run 5, the purity of BSA in the extract remained at 99.9+% with recovery increasing to 99.4% when accounting for material balance closure, and the purity of EHM in the extract increased to 97.8% with a recovery of 99.8%. Obtaining EHM with 97.8% purity at high recovery is a particularly significant result when considering that EHM comprised only 20% of the feed protein. The results of Runs 2–5 illustrate just how sensitive SMB performance can be to small changes in flow rates within each zone. In Run 6, the feed concentration was tripled while keeping all system flow rates and the step time the same as those used in Run 5. Similar product purities and recoveries were achieved. In Run 7, the SMB system productivity was increased further by doubling the feed rate. The results from Run 7 were again very good with BSA purity remaining at 99.9% with greater than 99% recovery. The EHM purity also remained high, dropping only slightly from previous runs to just less than 95% with higher than 99% recovery. We have also included results obtained after continuing Run 7 for an additional 24 h (Table 4). The process performance was very similar to the previous results, indicating that steady cyclical operation had been achieved at the earlier point in the run and that there was no significant fouling of the separation media during the course of a run.

Productivity

Table 5 lists productivities for each of the 7 miniplant runs. Productivities based on total packed-bed volume and total solvent use were as high as 1.74 g total product (isolated BSA plus isolated EHM) produced per hour per liter of media, and 3.7 g total product produced per liter of feed plus elution solvent. The concentration of protein in the feed was as high as 30 g/L total protein (80% BSA, 20% EHM). The dilution factors for each protein were about 4:1. By way of comparison, this productivity is significantly greater than that demonstrated by Houwing et al.[20] It should be emphasized, however, that these authors were first to develop the separation, and they did not claim to have optimized the SMB process for high productivity operation in their experiments. We calculate productivities for this earlier work of up to $P_{\text{media}} = 0.8$ g/h/L and $P_{\text{solvent}} = 0.3$ g/L. Dilution factors varied from 9:1 to 14:1 for a feed containing 6 g/L total protein (83.3% BSA, 16.7% EHM).

Table 3. SMB Miniplant Operating Conditions

Run	Feed (mL/min)	Eluent (mL/min)	Extract (mL/min)	Raffinate (mL/min)	BSA Feed Conc. (g/L)	EHM Feed Conc. (g/L)	Step Time (min)
Run 1 target*	0.5	3.3	2.4	1.4	8.0 ± 0.1	2.0 ± 0.02	13.0
Run 1 actual†	0.48 ± 0.02	3.18 ± 0.1	2.24 ± 0.05	1.43 ± 0.05	8.0 ± 0.1	2.0 ± 0.02	13.0
Run 2	0.45 ± 0.02	3.18 ± 0.1	2.24 ± 0.05	1.40 ± 0.05	8.0 ± 0.1	2.0 ± 0.02	14.0
Run 3	0.49 ± 0.02	3.18 ± 0.1	2.25 ± 0.05	1.43 ± 0.05	8.0 ± 0.1	2.0 ± 0.02	15.0
Run 4	0.49 ± 0.02	3.18 ± 0.1	1.94 ± 0.05	1.73 ± 0.05	8.0 ± 0.1	2.0 ± 0.02	15.0
Run 5	0.49 ± 0.02	3.56 ± 0.1	1.93 ± 0.05	2.12 ± 0.05	8.0 ± 0.1	2.0 ± 0.02	14.4
Run 6	0.49 ± 0.02	3.60 ± 0.1	1.96 ± 0.05	2.13 ± 0.05	24.0 ± 0.2	6.0 ± 0.05	14.4
Run 7	0.98 ± 0.03	7.12 ± 0.15	3.82 ± 0.05	4.26 ± 0.05	24.0 ± 0.2	6.0 ± 0.05	7.2

*Target conditions estimated from pulse test data (Figure 2).
†Conditions obtained after minor adjustments made during the run.

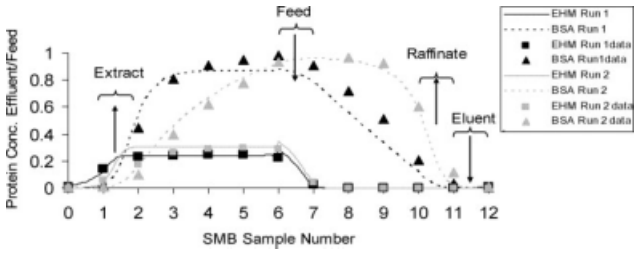

Figure 3. Miniplant data (symbols) and simulation results (lines) for Runs 1 and 2.

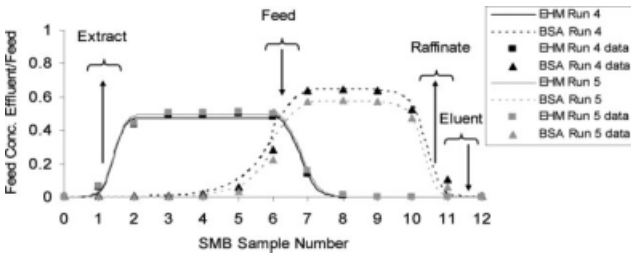

Figure 5. Miniplant data (symbols) and simulation results (lines) for Runs 4 and 5.

Pressure drop

The performance summarized in Tables 4 and 5 was achieved using total system pressures up to 580 psig (40 bar). This maximum pressure drop was due to flow through 5 columns. Lower pressures could be used in a commercial-scale unit by placing booster pumps after each column. This would yield pressure drops on the order of 120 psig (8 bar) per column based on the miniplant data. Although operation at significantly higher pressure drop might further increase productivity, we generally favor limiting pressure drop to this level to avoid high capital costs because of the high cost of large-scale equipment with a high pressure rating.[8] Pressure drop may also be reduced by operating at a higher temperature.

Process simulation results

The lumped-parameter model described by Eqs. 10–22 was developed to model the BSA/EHM protein separation by fitting the miniplant data from Run 3 (Figure 4). Effective overall values for the isotherm constants and mass transfer coefficients were determined by using the two-step procedure described earlier. All remaining model parameters were estimated from knowledge of the system. The final best-fit model parameters are summarized in Table 6. This set of parameter values was used to simulate all subsequent runs carried out over a wide range of operating conditions—without readjusting any of the values. Plots comparing simulation results with experimental process concentration profiles are shown in Figures 3–6 for Runs 1–7. The agreement between the simulation results and the overall set of process data is excellent with only slight deviations for Runs 1 and 7. Run 1 was a shakedown run that may not have attained completely steady cyclical operation. The Run 7 data set represents the greatest extrapolation away from the data set used to develop the model, to much higher solute concentrations and flow rates, yet the fit to the data remains quite good.

Calculated product composite concentrations were obtained by integrating the component profiles over the portion of the profile where the extract and raffinate streams leave the process. These results, summarized in Table 4, show that our process-data based approach to developing a simulation of the SMB process provides a good framework for representing trends in component concentrations and purities over a wide range of operating conditions.

Recommended methodology and example predictions

Methodology. Based on the previous discussion, we recommend the following procedures for evaluating a new SMB chromatography application and developing a process model from miniplant data:

(1) Use single-column pulse tests to screen various types of media and media properties (such as particle size, porosity, and pore structure), as well as a range of operating conditions such as temperature, elution solvent, or pH (if applicable).

(2) For the better performing candidate media, solvent, and temperature, analyze the pulse test chromatograms using the logic summarized in Table 1 to determine f_k values.

(3) Use these factors to specify initial conditions for an SMB miniplant test, as described in Table 1.

(4) After one or two shake-down runs, utilize miniplant data (typically expressed in terms of process concentration profiles as in Figure 4) to develop the lumped-parameter model described by Eqs. 10–22. Determine a value for ε_b from measurements for a given column or choose an approximate value for ε_b equal to 0.35 for spherical media or 0.45 for irregularly shaped media. To calculate initial values for ψ_i, utilize Eq. 12 with values for ε_p and $F_{se,i}$ obtained from measurements or by comparison with known values for similar media. Identify an approximate average particle size

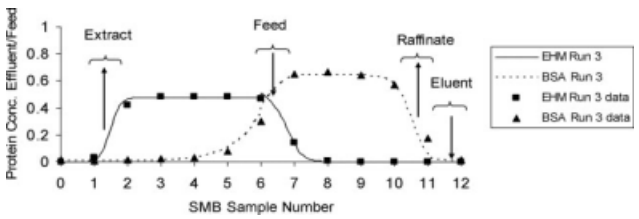

Figure 4. Miniplant data (symbols) used to develop the process model (lines).

The data are from Run 3. Final model parameters are summarized in Table 6.

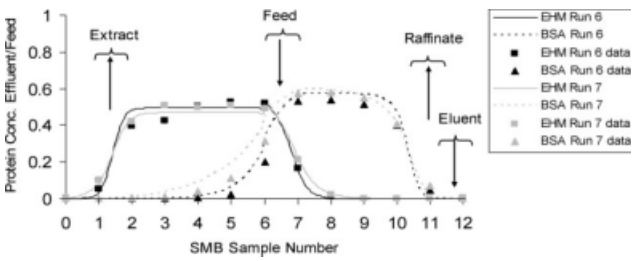

Figure 6. Miniplant data (symbols) and simulation results (lines) for Runs 6 and 7.

Table 4. SMB Miniplant Data and Simulation Results at Steady Cyclical Operation*

Run No. and change from previous run	Raffinate		Extract		% of Protein in Feed Recovered in the Desired Stream		Experimental Material Balance Accountability†	
	BSA Conc. (g/L)	BSA Purity‡ (%)	EHM Conc. (g/L)	EHM Purity‡ (%)	BSA in Raffinate (%)	EHM in Extract (%)	BSA (%)	EHM (%)
1. Initial run	0.75 ± 0.02	99.6	0.43 ± 0.01	25.6	27.6 (27.5)§	100.4 (99.6)§	100.4	100.8
	0.25	*98.5*	*0.44*	*20.2*	*9.0*	*97.6*		
2. Adjust f_k values to improve separation	2.36 ± 0.05	99.95	0.42 ± 0.01	61.9	91.9 (85.3)§	104.0 (99.9+)§	107.8	104.0
	1.73	*99.99*	*0.42*	*51.8*	*63.0*	*97.5*		
3. Adjust f_k values to improve separation	2.82 ± 0.05	99.95	0.43 ± 0.01	81.1	102.7 (94.7)§	99.4 (99.9)§	108.5	99.5
	2.65	*99.99*	*0.45*	*94.7*	*96.8*	*101.9*		
4. Adjust f_k values to improve separation	2.35 ± 0.05	99.95	0.53 ± 0.02	93.6	104.1 (98.3)§	104.2 (99.9)§	105.9	104.3
	2.32	*99.96*	*0.51*	*98.8*	*102.6*	*101.6*		
5. Adjust f_k values to improve separation	1.88 ± 0.05	99.95	0.53 ± 0.02	97.8	101.9 (99.4)§	103.4 (99.8)§	102.5	103.6
	1.84	*99.89*	*0.51*	*99.8*	*99.5*	*101.2*		
6. Triple feed concentration	5.27 ± 0.1	99.95	1.48 ± 0.03	97.5	95.5 (99.4)§	99.0 (99.9)§	96.1	99.1
	5.57	*99.89*	*1.55*	*99.8*	*100.9*	*103.3*		
7A. Double feed rate	5.54 ± 0.1	99.90	1.62 ± 0.03	94.6	100.4 (98.6)§	105 (99.6)§	101.8	105.6
	5.39	*98.90*	*1.49*	*92.0*	*97.6*	*96.7*		
7B. Validate steady operation‖	5.54 ± 0.1	99.90	1.56 ± 0.03	94.7	100.1 (99.5)§	101.2 (99.6)§	101.6	101.5
	5.39	*98.90*	*1.49*	*92.0*	*97.6*	*96.7*		

*Simulation results obtained using the model summarized in Table 6, shown in italics.
†$100 \times [C_{i,\text{raff}}Q_{\text{raff}} + C_{i,\text{extract}}Q_{\text{extract}}]/C_{i,\text{feed}}Q_{\text{feed}}$.
‡Calculated from measured BSA and EHM concentrations.
§Recovery adjusted to force ~100% material balance: $\text{Recovery}_{\text{adjusted}} = 100 \times \text{Recovery}_{\text{initial}}$/experimental accountability (%).
‖Run 7 results after an additional 24 h of operation.

from knowledge of the particle size distribution. Calculate values for $D_{m,i}$ by using available correlations such as those given by Eqs. 23 and 24. (Other ways of estimating initial values of mass transfer coefficients and ψ_i might also be used if available.) Starting with these initial estimates of ψ_i, determine effective values for K_i by using standard fitting routines to fit the miniplant data, treating the isotherm constants as adjustable parameters. If needed, the fit to the data may be improved in a second fitting step, this time adjusting the ψ_i values and holding the K_i values constant. This second adjustment can be particularly effective at improving the fit to the leading and trailing edges of the process concentration profiles. Subsequent adjustment of K_i values or ε_b may further improve the fit; however, this additional step was not necessary in our example. Chan et al.[42] provide additional guidance regarding strategies for adjusting model parameters to fit chromatography data.

(5) Keeping in mind the flow rate requirements outlined in "Key Process Concepts," use model calculations to identify changes in flow rates within each zone that move the process operation toward higher productivity while maintaining raffinate and extract compositions within desired specifications. Also consider the potential effects that using higher feed concentrations, higher feed rates, and lower solvent rates might have on the productivity of the process. This will be an iterative work process in which a change in one process variable such as feed concentration may require readjustment of the flow rates within each zone to maximize productivity or to maintain product purity and recovery.

(6) Run additional miniplant experiments as needed to test the predictions and demonstrate performance. If necessary, adjust the model parameter values to improve the fit to the most promising miniplant run, and repeat Step 5.

(7) Once the conditions for a final design have been chosen, model parameters may be adjusted again to optimize the model's ability to represent process performance at the design conditions. Then, the resulting dynamic simulation may be used to help specify the commercial design as well as to help develop start-up and control strategies.

As our example has demonstrated, this methodology can yield a mathematical model that provides a good fit to miniplant data over a wide range of operating conditions. To be

Table 5. SMB Process Productivities and Dilution Factors

Run No.	P_{media} (g/h/L)			P_{solvent} (g/L)			F_{dilution}	
	BSA	EHM	Total Protein	BSA	EHM	Total Protein	BSA	EHM
1	0.06	0.056	0.12	0.29	0.26	0.56	10.7	4.7
2	0.19	0.055	0.25	0.91	0.26	1.2	3.4	4.8
3	0.24	0.056	0.30	1.10	0.26	1.4	2.8	4.7
4	0.24	0.060	0.30	1.11	0.28	1.4	3.4	3.8
5	0.23	0.060	0.29	0.98	0.25	1.2	4.2	3.8
6	0.66	0.17	0.83	2.8	0.71	3.5	4.6	4.1
7A	1.38	0.36	1.74	2.9	0.76	3.7	4.3	3.7
7B*	1.38	0.35	1.73	2.9	0.74	3.7	4.3	3.8

*Run 7 results after an additional 24 h of operation.

Table 6. Process Model Parameter Values Obtained by Fitting Run 3 Data

Best-fit linear adsorption isotherm constants*	$K_{EHM} = 1.14$ $K_{BSA} = 0.79$
Columns per zone (2-5-4-1 configuration)	Zone I = 2 columns Zone II = 5 columns Zone III = 4 columns Zone IV = 1 column
Flow rates (mL/min) and step time	Values listed in Table 3
Solute concentrations in the feed (g/L)	Values listed in Table 3
Fixed-bed voidage and intraparticle porosity	$\varepsilon_b = 0.35$, $\varepsilon_p = 0.92$
Mass transfer coefficients (final values).* Initial values of ψ_i were estimated using Eqs. 12 and 23.	$k_{m,EHM}\, a_p = 2.1\ min^{-1}$ $k_{m,BSA}\, a_p = 1.0\ min^{-1}$
Size exclusion factors	$F_{se} = 0.83$ for EHM $F_{se} = 0.70$ for BSA
Axial dispersion coefficients† (cm^2/min) for Runs 1 to 6	$E_1 = 0.40$ $E_2 = 0.28$ $E_3 = 0.30$ $E_4 = 0.23$
Axial dispersion coefficients† (cm^2/min) for Run 7	$E_1 = 0.77$ $E_2 = 0.57$ $E_3 = 0.63$ $E_4 = 0.40$
Effective particle diameter (μm)	$d_p = 175$
Liquid density (g/mL)	$\rho = 1.0$
Liquid viscosity (Cp)	$\mu = 0.89$

*Obtained using the two-step procedure described in Process Simulation.
†Calculated using Eq. 22.

successful, the methodology requires generation of reliable process data, so careful attention to accurate measurement of concentrations, flow rates, and component accountabilities is needed. Uncertainties in the process data used to develop the simulation can have a large impact on the simulation's ability to extrapolate performance to untried operating conditions.

Because the methodology produces a reliable simulation of the process, Step 5 allows rapid consideration of many potential changes in process variables and for this reason can save much time in process development. Furthermore, computational approaches may be used to facilitate optimization of the process. An example is discussed by Kawajiri and Biegler.[30] Careful attention to computational efficiency will be needed because of long computation times required for accurate simulation using a rate-based model. Computation time may be reduced using various numerical methods such as the wavelet collocation method described by Yao et al.[50]

As discussed earlier, the lumped-parameter linear driving force model given by Eqs. 10–22 involves a number of simplifying assumptions. Once a set of model parameters has been determined by fitting data from an early miniplant run, and a given process moves toward higher and higher productivity, at some point the deviation between model predictions and actual performance is likely to increase (as discussed earlier for Run 7 in Figure 6). This may occur because nonlinear effects begin to be felt as solute concentrations increase. However, the ability of the lumped-parameter model to guide miniplant experimentation may be extended simply by refitting the data to determine new effective values for K_i and ψ_i that better match the latest process data, thus anchoring the model at a better position from which to extrapolate further. An example is illustrated in Figure 7, which shows the improved fit achieved by refitting the Run 7 data. In this particular case, the deviation was small and refitting the data was not necessary to obtain a good representation of process performance (as shown in Table 4). In practice, however, updating the model parameters as more process data become available at higher levels of productivity is recommended to insure the best possible representation.

The methodology we describe does not include specific reference to identifying an optimal particle size; however, Steps 1–6 can be used to evaluate a range of particle characteristics including particle size. The effect of particle size could be included in the simulation by noting that $\psi_i \propto 1/d_p^2$ and by adding an expression for pressure drop as a function of particle size and face velocity, treating particle size as an adjustable process variable. In principle, the model could then be used to identify the proper balance between particle size, face velocity, and column length in order to maximize separation performance without exceeding a practical pressure drop limit. In our example using the BSA/EHM model system, we utilized media with a size distribution of 100–250 μm in diameter, close to the 145 μm diameter that Houwing et al.[20] claimed should be the optimal particle size for this system using a similar media. In general, media in this size range can provide a good balance of desirable properties in terms of achieving good separation performance using relatively long columns without excessive pressure drop.[8] Temperature also is an important factor because of its potential impact on diffusivities, adsorption constants, and pressure drop. Initial pulse tests including pressure drop measurements can be carried out to determine the most effective operating temperature.

Finally, we have focused our work on increasing the productivity of a traditional SMB process scheme. The same approach also may be applied to other SMB process schemes described in the literature.[9] Once a satisfactory process simulation has been developed for a given process scheme, it is possible to estimate the relative performance of alternative process schemes by changing the details of the code (introducing different boundary conditions, variable feed concentrations, or variable switching times, for example) to model the alternative configuration.

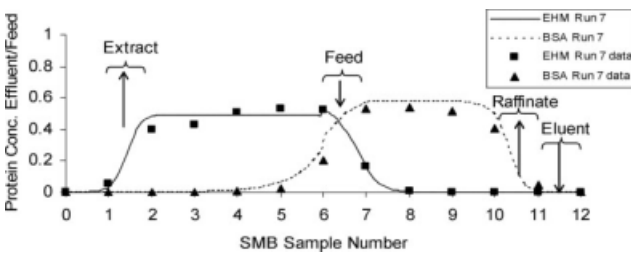

Figure 7. Simulation results achieved after refitting the Run 7 data in Figure 6.

Best-fit model parameters are $K_{BSA} = 0.78$, $k_{m,BSA}\, a_p = 2.1\ min^{-1}$, all else the same as in Table 6.

Table 7. Predictions of Overall SMB Performance for the Model Protein System*

Case	Process Change	Purity (%)		Recovery (%)		P_{media} (g/h/L)		$P_{solvent}$ (g/L)		$F_{dilution}$	
		BSA	EHM	BSA	EHM	BSA	EHM	BSA	EHM	BSA	EHM
Run 7 for comparison	Experiment	99.9	94.6	98.6	99.6	1.38	0.36	2.9	0.76	4.33	3.70
	Simulation (Tables 4 and 5)	98.9	92.0	97.6	96.7	1.34	0.33	2.84	0.70	4.45	4.03
A	Increase the feed rate by 50%.†	99.0	94.6	96.7	97.9	1.99	0.50	3.97	1.00	3.36	2.65
B	Increase the total protein concentration in the feed by 50%.	99.0	94.2	96.4	97.9	1.98	0.50	4.21	1.07	4.51	3.98
C	Add one column to Zone II and one column to Zone III to obtain zone configuration 2-6-5-1.‡	99.3	95.0	96.7	98.7	1.14	0.29	2.82	0.72	4.49	3.95
D	Reduce the elution solvent addition rate by 20%.§	96.7	93.5	96.4	88.6	1.32	0.30	3.40	0.78	4.51	2.76
E	Reduce elution solvent addition rate by 20%, use zone configuration 2-6-3-1 with a slightly increased step time from 7.20 to 7.25 min.‡,§	96.9	97.8	97.4	89.0	1.34	0.31	3.44	0.79	4.46	2.75

*Calculated using model parameter values listed in Table 6.
†The raffinate outflow was increased to accommodate the increase in feed flow rate. The extract flow rate was kept the same as in Run 7.
‡Each column was equal in size to the columns used for Run 7.
§The extract outflow was reduced to accommodate the decrease in the elution solvent addition rate. The raffinate flow rate was kept the same as in Run 7.

Example Predictions. Table 7 lists the results of predictions calculated using the process model summarized in Table 6 to illustrate how the methodology can be used to assess trends and guide experimentation. As described in Table 7, each case considers the impact of making specific changes relative to Run 7 as a base case, all else the same. These examples illustrate the effect of a change in a single variable. Multi-variable optimization likely will yield improved results.

Case A illustrates the potential impact of an increase in the feed rate. In this example, the elution solvent inlet rate is not changed, so both product dilution factors decrease significantly as the feed rate increases, by a factor of 1.3 for BSA produced in the raffinate and 1.5 for EHM in the extract. Yet the calculations suggest that very similar purities and recoveries can be achieved. Compared to the calculation results for Run 7, the results for Case A indicate somewhat higher EHM purity and recovery at the expense of only a slight reduction in BSA recovery.

Case B considers the effect of pre-concentrating the feed to achieve a 50% increase in the concentration of solute entering the SMB process. Media and solvent productivities increase relative to the Run 7 baseline because of increased solute concentrations for the same solvent and media usage. The purities and recoveries predicted for Case B are essentially the same as those calculated for Case A, but the dilution factors are somewhat higher. As a result, the concentrations of products in the raffinate and extract are similar; Case B predicts 7.98 g/mL BSA in the raffinate versus 7.14 g/mL for Case A, and both cases yield the same EHM concentration in the extract (2.26 g/mL). This suggests that a concentration effect almost equal to that achieved by preconcentrating the feed prior to SMB processing can be achieved by simply increasing the feed rate to the SMB process. This is an interesting result that could be explored further in optimizing an overall process design.

Case C considers the improvement that might result by adding additional equal-volume columns to each of Zones II and III to obtain a 14 column system with a 2-6-5-1 zone configuration. The total media-filled column volume is then 1/6 larger than the base case, so productivities measured in terms of media utilization decline, while the purities of both products increase slightly. Compared to the base case, the simulation predicts somewhat reduced BSA recovery and higher EHM recovery.

Case D illustrates how performance might change on reducing the amount of elution solvent by 20%. The raffinate flow rate was kept the same as in Run 7, so the dilution factor for BSA isolated in the raffinate remained essentially unchanged, while that for EHM isolated in the extract was significantly reduced. The simulation predicts a reduction in the recovery of each product in their respective product streams (the reduction in recovery is particularly large for EHM), with a reduction in the purity of BSA and a slight increase in the purity of EHM.

Case E is targeted toward a scenario where high EHM product purity is needed, despite the low purity of the EHM in the feed. By specifying a 2-6-3-1 zone configuration, more media are used in the zone that allows BSA to move forward and further away from EHM (Zone II). With a slight increase in step time to enhance this effect, this set of operating conditions achieves the highest EHM purity of any of the simulations. However, compared to the Run 7 baseline, the increase in EHM purity is obtained at the expense of a loss in EHM recovery and a slight decrease in BSA purity.

Summary

We have proposed a systematic approach to rapid evaluation of new applications of SMB chromatography and rapid development of an accurate design model. The methodology involves the use of single-column pulse-tests, SMB miniplant experiments, and process simulation using a lumped-parameter linear driving force rate-based model. Pulse tests are first used to screen media and other operating conditions such as solvent composition and temperature and to determine values of profile advancement factors to use in estimating initial flow rates for a subsequent miniplant run. A rate-based simulation of miniplant performance is then developed by fitting data from a single miniplant run in a two-step

procedure. In the first step, effective values of linear adsorption isotherm constants are determined by treating them as adjustable model parameters. All other model input values including mass transfer coefficients are estimated from knowledge of the system or from available correlation equations. In the second step, the fit to the data is fine tuned by adjusting the mass transfer coefficients, keeping all other model parameter values constant. For good results, care must be taken when generating miniplant data to accurately measure liquid flow rates, because SMB performance and simulation results are highly sensitive to changes in the flow rates within each zone. The resulting simulation can then be used to guide subsequent experimentation aimed at achieving further improvements in performance, refitting the model parameters if needed as more process data become available. The same methodology could be utilized to fit process data from an existing commercial operation to evaluate options for improving performance.

To evaluate and illustrate the methodology, we generated well-characterized miniplant data demonstrating high productivity operation using a model protein system and size-exclusion media. As a measure of process performance, productivities based on total packed-bed volume and total solvent volume were tracked for each miniplant experiment. A dilution factor was also defined to quantify the extent to which an SMB process dilutes products relative to their concentration in the feed. The proposed methodology was evaluated by fitting the rate-based model to data from a single miniplant run. Without further adjustment of the fitting parameters, the model yielded an excellent representation of process concentration profiles and data trends measured in four subsequent runs covering a wide range of operating conditions, including the impact of significant increases in feed rate and feed concentrations. The same methodology should be useful for developing other SMB chromatography applications, as well.

Acknowledgments

The authors gratefully acknowledge David Albers and Richard Stringfield for valuable discussions; Aaron Smalley and Peter Vargas, II for help with the SMB miniplant; Dee Dickerson for computer hardware; and Daniel Hickman and Michael Caracotsios for advice regarding general aspects of process simulation using Athena® Visual Studio.

Notation

a_p = external surface area per unit volume of a particle (cm^2/cm^3)
A = the key fast eluting solute produced in the raffinate
B = the key slow eluting solute produced in the extract
BV_j = number of empty bed volumes of feed liquid that have passed through column j
C_{ij} = concentration of component i in column j (g/L)
$C_{ij,0}$ = concentration of component i in column j at $x = 0$ (g/L)
$C_{i,raff}$ = concentration of component i (A or B) in the raffinate (g/L)
$C_{i,extract}$ = concentration of component i (A or B) in the extract (g/L)
$C_{i,feed}$ = concentration of component i (A or B) in the feed (g/L)
d_p = average or effective particle diameter (μm or cm)
$D_{eff,i}$ = intraparticle (effective) diffusion coefficient for component i (cm^2/s)
$D_{m,i}$ = molecular diffusion coefficient for component i in dilute liquid solution (cm^2/s)
E_j = axial dispersion coefficient for column j (cm^2/s or cm^2/min)
f_k = profile advancement factor for Zone k
$F_{dilution,A}$ = dilution factor for product A produced in the raffinate (no units)
$F_{dilution,B}$ = dilution factor for product B produced in the extract (no units)
$F_{se,i}$ = size exclusion factor for component i (no units)
$k_{m,i}$ = media overall or lumped-parameter mass transfer coefficient, for i (cm/s or cm/min)
$k_{ext,i}$ = mass transfer coefficient for external film resistance, for i (cm/s or cm/min)
$k_{int,i}$ = mass transfer coefficient for intraparticle resistance, for i (cm/s or cm/min)
K_i = effective isotherm constant for component i (mass per unit volume basis, no units)
L = column length (cm)
P_{media} = productivity with respect to the amount of media used (g/h/L)
$P_{solvent}$ = productivity with respect to the amount of feed and elution solvent used (g/L)
Pe = Peclet number ($d_p\ u_j/E_j$)
q_{ij} = conc. of component i adsorbed within a solid particle in column j (g/L)
q_{ij}^{eq} = equil. conc. of component i adsorbed within a solid particle in column j (g/L)
Q_{eluent} = volumetric flow rate of elution solvent added to the process (L/min)
$Q_{extract}$ = volumetric flow rate of extract (L/min)
Q_{feed} = volumetric flow rate of feed entering the process (L/min)
Q_k = volumetric flow rate within Zone k (L/min)
Q_{raff} = volumetric flow rate of raffinate (L/min)
Q_I = volumetric flow rate within Zone I (L/min)
Q_{II} = volumetric flow rate within Zone II (L/min)
Q_{III} = volumetric flow rate within Zone III (L/min)
Q_{IV} = volumetric flow rate within Zone IV (L/min)
Re = Reynolds number ($d_p\ u\rho/\mu$)
t = elapsed time (s or min)
t_{step} = step time between switching of flows in the SMB cycle (min)
T = absolute temperature (K)
u_j = superficial liquid velocity (or face velocity) in column j (cm/min)
V_{column} = total volume of a column plus fittings (L)
V_{media} = total bulk volume of media used in the SMB process (L)
$V_{m,i}$ = liquid molar volume of component i at its normal boiling point (mL/g-mol)
$V_{m,liquid}$ = molar volume of bulk liquid phase at its normal boiling point (mL/g-mol)
x = axial distance coordinate (cm)
ε_b = interparticle porosity (fixed-bed voidage) (no units)
ε_p = intraparticle porosity (no units)
μ = viscosity of liquid phase (g/cm/s or cP)
ρ = density of liquid phase (g/mL)
ψ_i = constant number in Eqs. 10–12, for component i (s^{-1} or min^{-1})

Literature Cited

1. Robbins LA. The miniplant concept. *Chem Eng Prog*. 1979;75:45–48.
2. Heimann F. Process intensification through the combined use of process simulation and miniplant technology. *Comput Aided Chem Eng*. 2003;14:155–160.
3. Ouni T, Lievo P, Uusi-Kyyny P, Dell'Era C, Jakobsson K, Pyhälahti A, Aittamaa J. Practical methodology for distillation design using a miniplant. *Chem Eng Technol*. 2006;29:104–112.
4. Fair JR, Seibert AF. Using an Oldershaw column for scale-up. *Chem Eng Prog*. 2008;104:27–29.
5. Heinrich ES, Deibele L, Schröter J. Miniplant engineering. Selected examples of equipment design. *Chem Ing Technik*. 1997;69:623–631.
6. Kolb P, Bart H-J, Fischer L. Development of a miniplant extraction column. *Chem Ing Technik*. 2002;74:243–247.
7. Frank TC, Dahuron D, Holden BS, Prince WD, Seibert AF, Wilson LC. Section 15. Liquid-liquid extraction and other liquid-liquid operations and equipment. In: Green DW. *Perry's Chemical Engineers' Handbook*, 8th ed. New York: McGraw-Hill, 2008.

8. Pynnonen BW. Simulated moving bed processing: escape from the high-cost box. *J Chromatogr A*. 1998;827:143–160.
9. Chin CY, Wang N-HL. Simulated moving bed equipment designs. *Sep Purif Rev*. 2004;33:77–155.
10. Kearney MM. Engineered fractals enhance process applications. *Chem Eng Prog*. 2000;96:61–68.
11. Augier F, Laroche C, Brehon E. Application of computational fluid dynamics to fixed bed adsorption calculations: effect of hydrodynamics at laboratory and industrial scale. *Sep Purif Technol*. 2008;63:466–474.
12. Shams A, Molaei Dehkordi A, Goodarznia I. Desulfurization of liquid-phase butane by zeolite molecular sieve 13X in a fixed bed: modeling, simulation, and comparison with commercial-scale plant data. *Energy Fuels*. 2008;22:570–575.
13. Broughton DB, Gerhold CG. Continuous sorption process employing fixed beds of sorbent and moving inlets and outlets. U.S. Pat., 2,985,589, 1961.
14. Ruthven DM, Ching CB. Counter-current and simulated counter-current adsorption separation processes. *Chem Eng Sci*. 1989;44:1011–1038.
15. Wankat PC. *Separation Process Engineering*, 2nd ed. Upper Saddle River, NJ: Prentice Hall, 2007: 649–654.
16. Minceva M, Rodriques AE. Understanding and revamping of industrial SMB units for *p*-xylene separation. *AIChE J*. 2007;53:138–149.
17. Azevedo DCS, Rodrigues AE. Fructose–glucose separation in a SMB pilot unit: Modeling, simulation, design, and operation. *AIChE J*. 2001;47:2042–2051.
18. Lefevre L. Separation of fructose from glucose using cation exchange resin salts. U.S. Pat., 3,044,905, 1962.
19. Lee H-J, Xie Y, Koo Y-M, Wang N-HL. Separation of lactic acid from acetic acid using a four-zone SMB. *Biotechnol Prog*. 2004; 20:179–192.
20. Houwing J, Billiet HAH, van der Wielen LAM. Mass-transfer effects during separation of proteins in SMB by size exclusion. *AIChE J*. 2003;49:1158–1167.
21. Li P, Xiu G, Rodrigues AE. Proteins separation and purification by salt gradient ion-exchange SMB. *AIChE J*. 2007;53:2419–2431.
22. Strube J, Jupke A, Epping A, Schmidt-Traub H, Schulte M, Devant R. Design, optimization, and operation of SMB chromatography in the production of enantiomerically pure pharmaceuticals. *Chirality*. 1999;11:440–450.
23. Wongso F, Hidajat K, Ray AK. Optimal operating mode for enantioseparation of SB-553261 racemate based on simulated moving bed technology. *Biotechnol Bioeng*. 2004;87:704–722.
24. Migliorini C, Mazzotti M, Zenoni G, Morbidelli M. Shortcut experimental method for designing chiral SMB separations. *AIChE J*. 2002;48:69–77.
25. Zhang Z, Hidajat K, Ray AK, Morbidelli M. Multiobjective optimization of SMB and VARICOL^{TM} process for chiral separation. *AIChE J*. 2002;48:2800–2816.
26. deRosset AJ, Neuzil RW, Korous DJ. Liquid column chromatography as a predictive tool for continuous countercurrent adsorptive separations. *Ind Eng Chem Process Des Dev*. 1976;15:261–266.
27. Charton F, Nicoud R-M. Complete design of a simulated moving bed. *J Chromatogr A*. 1995;702:97–112.
28. Migliorini C, Gentilini A, Mazzotti M, Morbidelli M. Design of simulated moving bed units under nonideal conditions. *Ind Eng Chem Res*. 1999;38:2400–2410.
29. Cauley FG, Xie Y, Wang N-HL. Optimization of SMB systems with linear adsorption isotherms by the standing wave annealing technique. *Ind Eng Chem Res*. 2004;43:7588–7599.
30. Kawajiri Y, Biegler L. Optimization strategies for simulated moving bed and PowerFeed processes. *AIChE J*. 2006;52:1343–1350.
31. Migliorini C, Mazzotti M, Morbidelli M. Continuous chromatographic separation through simulated moving beds under linear and nonlinear conditions. *J Chromatogr A*. 1998;827:161–173.
32. Grznárová G, Yu S, Štefuca V, Polaković M. Quantitative characterization of pore structure of cellulose gels with or without bound protein ligand. *J Chromatogr A*. 2005;1092:107–113.
33. Grosfils V, Levrie C, Kinnaert M, Vande Wouwer A. On simplified modeling approaches to SMB processes. *Comput Chem Eng*. 2007; 31:196–205.
34. Pais LS, Loureiro JM, Rodrigues AE. Modeling strategies for enantiomers separation by SMB chromatography. *AIChE J*. 1998;44:561–569.
35. Ruthven DM, Farooq S, Knaebel KS. *Pressure Swing Adsorption*. New York: VCH, 1994:60.
36. Kaczmarski K, Antos D, Sajonz H, Sajonz P, Guiochon G. Comparative modeling of breakthrough curves of bovine serum albumin in anion-exchange chromatography. *J Chromatogr A*. 2001;925:1–17.
37. Ladisch MR. *Bioseparations Engineering. Principles, Practice, and Economics*. New York: Wiley, 2001.
38. LeVan MD, Carta G. Section 16. Adsorption and ion exchange. In: Green DW. *Perry's Chemical Engineers' Handbook*, 8th ed. New York: McGraw-Hill, 2008.
39. Migliorini C, Mazzotti M, Morbidelli M. Simulated moving-bed units with extra-column dead volume. *AIChE J*. 1999;45:1411–1421.
40. Chung SF, Wen CY. Longitudinal dispersion of liquid flowing through fixed and fluidized beds. *AIChE J*. 1968;14:857–866.
41. Siddiqi M, Lucas K. Correlations for prediction of diffusion in liquids. *Can J Chem Eng*. 1986;64:839–843.
42. Chan S, Titchener-Hooker N, Bracewell DG, Sørensen EA. Systematic approach for modeling chromatographic processes—application to protein purification. *AIChE J*. 2008;54:965–977.
43. Seidel-Morgenstern A. Experimental determination of single solute and competitive adsorption isotherms. *J Chromatogr A*. 2004;1037: 255–272.
44. Caracotsios M. Athena visual studio version 11. Process modeling and parameter estimation: technical and user guide. 2006. Available at: www.athenavisual.com.
45. Stewart, WE, Caracotsios M. *Computer-Aided Modeling of Reactive Systems*. Hoboken, NJ: Wiley, 2008.
46. Liu X-D, Osher S, Chan T. Weighted essentially non-oscillatory schemes. *J Comput Phys*. 1994;115:200–212.
47. Minceva M, Pais LS, Rodrigues AE. Cyclic steady state of simulated moving bed processes for enantiomers separation. *Chem Eng Process*. 2003;42:93–104.
48. Xin Y, Whiting WB. Case studies of computer-aided design sensitivity to thermodynamic data and models. *Ind Eng Chem Res*. 2000;39:2998–3006.
49. Pynnonen BW. Engineering design and characterization of pseudo-moving bed processes. In: *211th ACS National Meeting*, New Orleans, March 24–28, 1996, paper I&EC-137.
50. Yao H, Tian Y-C, Tade MO. Using wavelets for solving SMB separation process models. *Ind Eng Chem Res*. 2008;47:5585–5593.

Manuscript received Oct. 8, 2008, and revision received Apr. 15, 2009.